# INORGANIC CHEMISTRY

## FRONTIERS

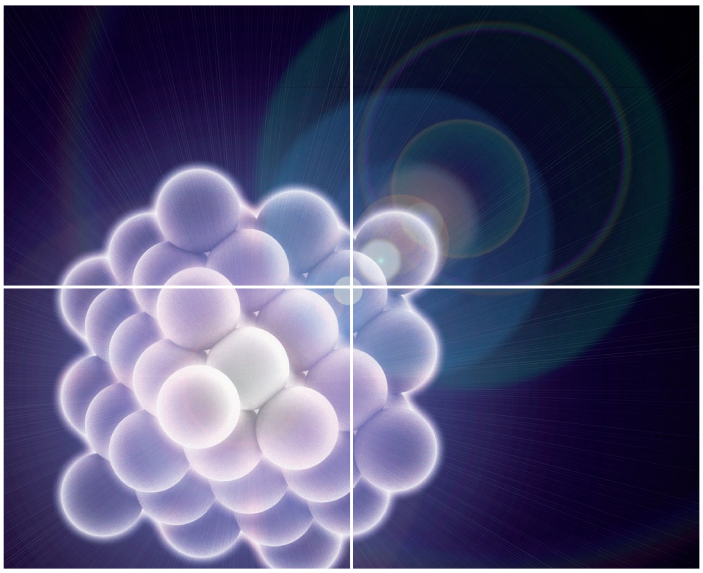

Accepted Manuscript

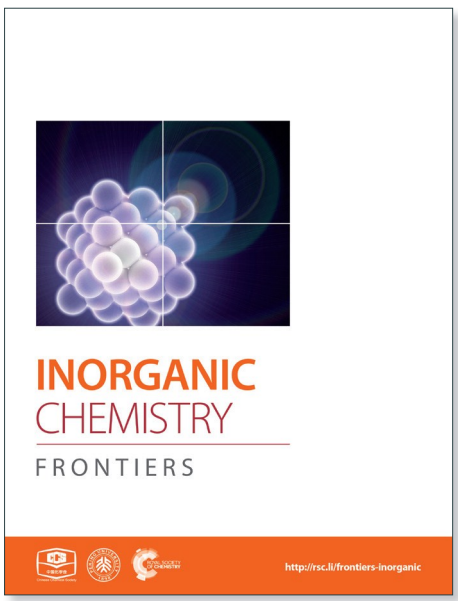


This is an *Accepted Manuscript*, which has been through the Royal Society of Chemistry peer review process and has been accepted for publication.

*Accepted Manuscripts* are published online shortly after acceptance, before technical editing, formatting and proof reading. Using this free service, authors can make their results available to the community, in citable form, before we publish the edited article. We will replace this *Accepted Manuscript* with the edited and formatted *Advance Article* as soon as it is available.

You can find more information about *Accepted Manuscripts* in the **Information for Authors**.

Please note that technical editing may introduce minor changes to the text and/or graphics, which may alter content. The journal's standard **Terms & Conditions** and the **Ethical guidelines** still apply. In no event shall the Royal Society of Chemistry be held responsible for any errors or omissions in this *Accepted Manuscript* or any consequences arising from the use of any information it contains.

**Invited Review Paper for *Inorganic Chemistry Frontiers***

# Intercalation in Two-Dimensional Transition Metal Chalcogenides

Yeonwoong Jung[1], Yu Zhou[2,3], Judy J. Cha[2,3,4]

1. Nanoscience Technology Center, Department of Materials Science and Engineering, University of Central Florida, Orlando, Florida 32826
2. Department of Mechanical Engineering and Materials Science, Yale University, New Haven, CT 06511
3. Energy Sciences Institute, Yale West Campus, West Haven, CT 06525
4. Center for Research on Interface Structures and Phenomena, Yale University, New Haven, CT 06511

CORRESPONDING AUTHOR FOOTNOTE:

*Corresponding author.
E-mail: judy.cha@yale.edu,
E-mail: yeonwoong.jung@ucf.edu

**Abstract**

Intercalation is a reversible insertion process of foreign species into crystal gaps. Layered materials are good host materials for various intercalant species ranging from small ions to atoms to molecules. Given the recent intense interest in two-dimensional (2D) layered materials in thin limits, this review highlights the opportunities that intercalation chemistry can provide for nanoscale layered materials. Novel heterostructures or emergent electrical properties not found in the intrinsic host materials are possible with intercalation. In particular, we review various exfoliation methods developed for 2D layered nanomaterials based on intercalation chemistry and extensive tuning of electrical, optical, and magnetic properties of 2D layered materials due to intercalation.

## 1. Brief history of intercalation into bulk transition metal chalcogenides

Bulk layered materials have been studied extensively in the past several decades because of their unique structural features, and physical and chemical properties [1]. The rich family of layered materials consists of single-element crystals, such as graphite, phosphorus, arsenic, antimony and bismuth, silicates, hydroxides, organic compounds such as rubrene ($C_{42}H_{28}$) and dioctylbenzothienobenzothiophene ($C_8$-BTBT), and inorganic compounds such as transition metal chalcogenides and many oxides [2-7]. Layered materials typically exhibit strong in-plane covalent boning and weak out-of-plane van der Waals interactions through the interlayer gap [8]. They exhibit a wide range of electronic band structures from insulators, semiconductors, metals, superconductors to topological insulators [8-11]. Here we limit ourselves specifically to transition metal chalcogenides, which are usually referred to as $MX_2$ and MX, where M represents a transition metal from group 4 to group 10 (such as Nb, Mo, Ti, V, Hf, Ta, W, Fe), and X represents the chalcogen (S, Se, and Te). Owing to the layered structure with a rather large interlayer gap, intercalation into the transition metal chalcogenides is easily achieved for fundamental studies as well as for technological applications (Figure 1) [12, 13].

Intercalation is a chemical process to reversibly insert foreign species at the crystal gap. Intercalation layered materials have been paid much attentions in the condensed matter physics and the electrochemical energy devices. In condensed matter physics, intercalating transition metal dichalcogenides (TMDs) with ions leads

to charge density waves, two-dimensional superconductitivy, and interesting phase transitions [14, 15]. The most well-known electrochemical energy device using intercalation is a Li-ion battery in which Li-ions are intercalated at the van der Waals gaps reversibly for charging and discharging. The field of intercalation in layered materials has grown dramatically since the appearance of a large class of graphite intercalation compounds [14]. Intercalation into TMDs has been successfully achieved by chemical vapor transport, electrochemical method, ion exchange, and oxide-reduction method, in which the guest species introduced into the van der Waals gaps can be atoms, ions and molecules [8, 16]. Intercalation can change the band filling state and the Fermi level, resulting in superconductivity, charge density waves and the Peierls instability. For example, Geballe *et al.* reported a large class of organic molecules-intercalated TMDs as new superconductors [17]. In addition, Prober *et al*. showed that the dimensionality of the superconductivity in $(Pyridine)_{1/2}TaS_2$ intercalation compounds is in accord with the qualitative predictions of the Lawrence-Doniach theory for weakly-coupled superconducting layers [18].

## 2. **Brief introduction of two-dimensional transition metal chalcogenides**

As the first atomically thin two-dimensional (2D) crystal composed of a $sp^2$-bonded carbon framework, graphene has been extensively studied and used as device platforms in the condense matter physics, chemistry and material sciences due to its fascinating properties such as ultrahigh mobility (~200,000 $cm^2/V$ s), amazing optical transparency (~97.7%), and high thermal conductivity (~5300 W/m K) [19]. Following

graphene, interests for 2D layered materials have rapidly grown, particularly for TMDs [20]. Several applications have been demonstrated using 2D TMDs such as field effect transistors based on monolayer $MoS_2$ [21], optoelectronic devices based on monolayer and few-layer $MoS_2$ and $WSe_2$ [22], piezoelectric devices based on odd-layer TMDs ($MoS_2$, $WS_2$, $MoSe_2$ and $WSe_2$) [23, 24] and electrochemical electrodes based on few-layer $MoS_2$ and $WS_2$ [25]. In the case of 2D TMDs (for example, $MoS_2$), indirect-to-direct bandgap transition property and valley physics emerge when the thickness decreases to a monolayer regime [26]. In addition, inversion symmetry can be broken when thinned down to a single atomic layer, exhibiting novel properties such as large second-order nonlinear susceptibility, valley-selective circular dichroism and piezoelectricity [23, 27, 28]. Polymorphism has also been observed in the 2D TMDs. Generally several crystal structures are possible for TMDs such as 1T, 1T', and 2H. 1T Phase TMDs are an excellent candidate for electrochemical catalysts because of their enhanced conductivity and reduced reaction free energy [29]. For example, vertically aligned TMD layers and graphene-TMD composites create high number of catalytically active edge sites, significantly enhancing the hydrogen evolution reaction performance [29-32]. By vertically stacking 2D materials with different bandgaps and work functions, van der Waals heterostructures can be achieved to tune its electrical properties. Field effect tunneling transistors are reported as the first application of such tunability, in which $MoS_2$ or $WS_2$ serves as a vertical transport barrier [33]. Graphene-$WS_2$-graphene vertical devices have been successfully demonstrated as a gate tunable photovoltaic device with high external quantum efficiency [34]. An

atomically sharp heterostructure formed by stacking two different TMDs, atomically thin layers of $WSe_2$ (p-type semiconductor) and $MoS_2$ (n-type semiconductor), has shown diode behavior at dark state and photovoltaic effect upon illumination [35]. Forming p-n heterostructures using monolayer TMDs in the lateral direction is important for atomically thin field effect transistors, inverters, operational unit and digital circuits. Using the electrostatic gate doping and chemical vapor deposition doping growth method, a $WSe_2$ based lateral p-n junction showed impressive electronic and optoelectronic properties [36, 37]. Intercalation reaction offers another degree of freedom to achieve novel 2D layered materials and redesign and improve materials properties. Intercalation chemistry is critical for the exfoliation of 2D TMDs, tuning the physical properties such as electricity, thermoelectricity and superconductivity, and phase change for catalyst applications.

## 3. Intercalation in 2D TMDs.

### 3.1 Intercalation methods for exfoliation of 2D TMDs

This section reviews intercalation methodologies for various 2D layered materials, while mainly focusing on intercalation-assisted exfoliations of 2D TMDs.

#### 3.1.1 Earlier approaches: oxidation-reduction chemistry

Historically, intercalations have been applied to 2D materials as means of exfoliating individual 2D layers from their bulk counterparts in large quantities. Exfoliation of 2D materials was initially developed for graphite, which involves the manual rubbing and peeling of bulk graphite [38]. However, such mechanical exfoliation suffers from

low-yield production of desired materials, thus technologically non-scalable. Following the successful demonstration of the mechanical exfoliation, liquid-based exfoliation of layered materials was developed [39-41]. Contrast to the mechanical exfoliation, liquid-based exfoliations present great advantages of versatility, scalability, and reliability for the mass production of 2D materials, thus compatible with industrial scale techniques. Intercalation chemistry plays a key role in a majority of the liquid-based exfoliation methods. The underlying principle for the intercalation-based exfoliation is in increasing the interlayer spacing between individual 2D layers by inserting foreign species. This will weaken the interlayer adhesion and reduce the energy barrier to exfoliation, thus eventually increase the accessible surface areas in 2D materials [40]. One of the earliest exfoliation methods based on intercalation was developed for graphite, which involves the oxidation-reduction chemistry. In this approach pioneered by Ruoff *et al.* [42], graphite is oxidized by oxidizers such as sulfuric acids, which results in the attachment of hydroxyl groups to the graphene basal plane, causing hydrophilic surfaces. Then the oxidized graphite is dispersed in solvents, which allows for the intercalation of water molecules and the subsequent separation of 2D layers – graphene oxide – due to the enhanced hydrophilicity. The dispersed graphene oxides are subsequently stabilized against re-aggregation by chemical reduction, which removes most of the oxide residuals. Layered crystals are particularly suitable for intercalation processes as they can strongly adsorb guest species into their van der Waals gaps between each layer, forming the basis of intercalation-based exfoliations of a variety of 2D

materials, including 2D TMDs [8]. A major drawback of this method is that it introduces a significant amount of chemical groups and structural defects on the exfoliated materials. Thus, the physical properties of graphene exfoliated *via* the oxidation-reduction intercalations are quite different from those of its pristine form [42, 43]. For example, the electrical conductivity of the graphene obtained *via* intercalation is generally lower than that of the mechanically exfoliated one due to the enhanced electrons scattering from the structural defects.

### 3.1.2 Organic materials-based ion exchange intercalation

Some intercalants can transfer charges to targeted layers, lowering the interlayer binding strength of 2D layers. In general, ion exchange intercalations are based on the fact that some layered materials contain cationic counterions in 2D layers which can be exchanged for protons for charge neutrality by being dissolved in solvents [40]. The intercalated 2D layers are then easily exfoliated by various physical means such as shear mixing or ultrasonic waves [8, 40]. Earlier works can be found with the exfoliation of layered metal oxides developed over decades ago [44, 45]. Recently, ion-exchange intercalations have widely been employed to exfoliate a variety of 2D materials including graphene and 2D TMDs. A few-layer graphenes have been exfoliated from graphite via the intercalation of ionic compounds such as iodine chloride (ICl) or iodine bromide (IBr) [46]. For the exfoliation of 2D TMDs, organics-based intercalants such as n-butyllithium have been initially developed and applied to exfoliate single-layer 2D $MoS_2$ [8, 47]. In these approaches, organic ions can be intercalated into

neutralized 2D interlayers by proton exchange, which leads to substantial swelling in between the 2D layers as in the case of water-intercalations for graphite [41]. Figure 2(a) illustrates a schematic for the ion-exchange intercalation. Efforts to increase the scalability of intercalated 2D TMDs have been continuously pursued and various alkyl amines are used as intercalants; these include n-butylamine (BA), n-octylamine (OA), ndodecylamine (DDA), and n-octadecylamine (ODA) [48, 49]. Ammonia ion-based intercalations have also been developed for the exfoliation of 2D $WS_2$ [50]. Recently, high-yield exfoliation of 2D TMDs has been developed by using hydrazine ($N_2H_4$) as an intercalant [51]. Bulk TMD crystals are expanded by reacting them with $N_2H_4$ in hydrothermal conditions, which is enabled by a redox rearrangement model in which part of the $N_2H_4$ is oxidized to $N_2H_5$ upon intercalation [51]. Expanded TMDs react with alkali naphthalenide solution, and then exfoliate to single layers in water. Figure 2 (b)-(d) illustrates a schematic for the $N_2H_4$ based intercalations of various TMDs. Despite their versatility, one major drawback of the ion exchange-based intercalation approaches is their high sensitivity to ambient conditions, which limits the number of species to be intercalated into 2D materials.

### 3.1.3 **Zerovalent chemistry intercalation**

The degree of intercalation in 2D materials is determined by many factors such as (1) physical size of intercalating species (2) charge stage of intercalating species, and (3) structural stability of hosting materials after intercalation. In many cases, the intercalation of 2D materials is driven by the tendency for retaining charge neutrality

[13]. This is enabled by either a change of the oxidation states or by the presence of atomic vacancies to accommodate the charge neutrality. Intercalation of alkali metals such as lithium is relatively facile due to their small sizes irrespective of charge states while the ionic nature of intercalant critically determines the extent of intercalation in many cases. In this respect, zerovalent intercalation methods recently developed by Cui and Koski offer following advantages uniquely suitable for the intercalation of 2D materials [13]; (1) It does not require a change in the oxidation state of hosting materials. This advantage allows for the intercalation of various zerovalent metals (e.g., Ag, Au, Co, Cu, Fe, In, Ni, Pd and Sn) into 2D TMDs and realize their superstoichiometric compositions [52]. (2) It does not disrupt the hosting 2D layered structures, thus allowing a high degree of intercalation. For example, nearly 60 atomic percent of zerovalant Cu has been intercalated into $Bi_2Se_3$ layered crystals [53, 54]. Figure 3(a) illustrates a schematic for the zervalent intercalation and Figure 3(b) shows a variety of superlattice patterns observed upon the intercalation of Cu into $Bi_2Se_3$. The intercalation reaction is typically carried out by incorporating metal element containing precursors (e.g., tetrakis (acetonitrile) copper (I) hexafluorophosphate for Cu intercalation) into source materials under reflux at elevated temperatures [53]. These methods have been further extended to intercalate various TMDs (e.g., $Sb_2Te_3$, $In_2Se_3$, GaSe) [53] and non-TMDs such as $MoO_3$ [55] as well as, incorporating dual metal elements into them [56]. Also, they have been employed not only for exfoliating 2D materials, but more focusing on tuning their various physical properties which will be discussed in details later in this Review.

### 3.1.4 Electrochemical intercalation

Electrochemical reactions mainly developed for lithium (Li) ion batteries or supercapacitors can be used to tune the electronic structure and chemical potential of 2D materials by intercalating ions. In these approaches, either cations or anions can be electrochemically intercalated into the van der Waals gap of 2D materials or reacted with 2D crystalline lattices themselves *via* simple electrochemical reaction [13]. One of the most extensively employed electrochemical approaches is the intercalation of a Li ion based on the following; for the case of $MoS_2$ intercalation, $Li + MoS_2 + e \leftrightarrow Mo + LiS_2$. Unlike the zerovalent intercalation approach, the intercalation is driven by the change of the redox state of hosting lattices. In general, the $Li^+$ electrochemical intercalation is performed in a test cell using a Li foil as the anode, Li hexafluorophosphate ($LiPF_6$) as the electrolyte, and layered materials to be intercalated as the cathode using galvanostatic discharge at a certain current density [57]. Figure 4(a) illustrates a schematic for the $Li^+$ electrochemical intercalation. These reactions often realize superlattice structures in layered materials by generating new types of vacancies through a complete filling of Li atoms as well as introducing phase transformations [13, 58]. In addition, they can realize specific structural phases in 2D TMDs. For example, electrochemical $Li^+$ intercalation leads to the formation of metallic (1T) phase in 2D $MoS_2$ which are initially composed of metallic (1T) and semiconducting (2H) phases [59, 60]. Such phase-specific transformations have not been achieved from any other synthetic approaches for 2D TMDs. In addition to the phase

and composition engineering, electrochemical Li+ intercalations have been widely used to exfoliate a large number of 2D materials, including $MoS_2$, $WS_2$, $TiS_2$, $TaS_2$, $ZrS_2$, and graphite [40, 57]. Figure 4(b) –(c) show the morphologies of single-layer $MoS_2$ exfoliated by the $Li^+$ electrochemical intercalation.

### 3.2 Intercalation for tuning 2D materials properties

In addition to exfoliating individual 2D layers, intercalation has also been widely used to alter the physical and chemical properties of 2D materials. This section reviews the applications of intercalations to engineering the physical properties of 2D TMDs.

#### 3.2.1 Catalytic activity

The chemical and electrochemical intercalation can tune the electronic structures of 2D TMDs, thus radically enhancing their chemical and physical reactivity for catalytic applications. Electrochemical intercalation can effectively shift the chemical potentials of 2D TMDs within a wide range, which is suitable for optimizing catalytic properties [61]. For example, $Li^+$ intercalated 2D $MoS_2$ have exhibited enhanced hydrogen evolution reaction (HER) [29, 62, 63] . In these cases, intercalated Li atoms transfer excess charge carriers to $MoS_2$, which increases its charge carrier density, thus conductivity [29, 61]. Also, structural phase transitions into more stable octahedral coordination occur to lower the electronic energy of the whole system [29, 61]. Consequently, the chemical potential of Li-intercalated $MoS_2$ shifts and HER performance is improved. In addition to the alteration of electronic structures, intercalations often alter the structural phases of 2D TMDs to be more suitable for

catalysts [25, 59, 64]. For example, electrochemical intercalation of $Li^+$ has been shown to transform the 2H (semiconducting) phase of 2D $MoS_2$ and $WS_2$ into 1T (metallic) phase, and such 1T-rich 2D TMDs have exhibited enhanced HER performance [25, 59, 60]. Figure 5(a) illustrates a schematic for the 2H-to-1T phase-transition of 2D $MoS_2$ upon $Li^+$ intercalation. The improved catalytic activity is attributed to the following two factors which are results of the phase transition; (1) enhanced charge carrier conductivity due to enhanced metallic phases (2) lowering of the reaction free energy from the release of strain in 1T which is built up from the phase transition. Such 2H-to-1T phase-transition was also observed in the intercalation of $MoS_2$ where organic molecules such as n-butyllithium intercalants were used [62]. Figure 5(b) shows an enhanced HER performance of 1T-rich $MoS_2$ over 2H-rich $MoS_2$ after intercalation by n-butyllithium. Moreover, $MoS_2$ anode electrodes with high capacity and stability were prepared by intercalation and exfoliation restacking processes [65]. Intercalations have also been demonstrated to enhance the catalytic activities of 2D TMD-based composite materials. For example, Xiao *et al.* reported $MoS_2$/polyethylene oxide nanocomposites anodes using exfoliated $MoS_2$ and demonstrated improved lithiation capacity and cyclic performance [66]. Liu et al. reported CdS/$MoS_2$ hybrids using hydrothermal reaction synthesized 1T phase $MoS_2$ showed giant enhancement of photocatalytic hydrogen evolution rate[67].

### 3.2.2. Electrical and optical properties

Intercalation into layered structures can change electrical and optical properties of hosting 2D materials. Earlier studies focused on the bulk forms of TMDs are recently revisited as their nanoscale counterparts are now extensively being developed [14]. Intercalation can introduce charge transfers in 2D TMDs. For example, 2D TMDs intercalated with transition metals and alkali metals have exhibited electrical properties greatly different from their pristine forms [61]. The charge transfer from the metal intercalation shifts the Fermi energy and increases the density of energy states at the Fermi level, thus increases the charge carrier density of 2D TMDs [61]. Metal intercalation also modifies the optical properties of hosting 2D materials. This is manifested by the change of optical transmission and interference, as in the case of Cu-intercalated chalcogenide nanomaterials. Pristine $Bi_2Se_3$ nanoribbons display silvery white color which turns orange upon intercalation of Cu [54]. Intercalation of $Bi_2Se_3$ nanoribbons with organic molecules such as pyridine also results in significant dielectric optical mode peak shifts [68]. In addition, Cu-intercalated, very thin 2D $Bi_2Se_3$ exhibits unusual enhancement of optical transmission and electrical conductivities [69]. Figure 6 show the enhanced optical transparency ((a), (b)) and electrical conductivity ((c), (d)) of 2D $Bi_2Se_3$ plates with varying layer thickness upon Cu intercalation. $Li^+$ intercalated, a few-layer graphene also displays significantly enhanced optical transmittance and electrical conductance [70]. Such enhanced optical transparency is attributed to the increase of the effective bandgap due to the increase of free electron density introduced by metal atoms [69]. In addition to the charge carrier transfer, intercalations can be applied to modulate the physical dimensions of van der Waals

interlayer gaps in 2D TMDs. Such change in the physical structures of 2D TMDs, in turn, results in altering their electrical and optical properties. For example, the intercalations of organic molecules have been known to significantly enlarge the interlayer spacing of layered materials in bulk forms [17]. This results in weakening of the bonding strength of 2D interlayers, thus makes them electrically behave more like isolated single layers. A similar behavior was observed in the electrochemical intercalation of $Li^+$ into 2D $MoS_2$ [29]. Figure 6 shows the gradual change of interlayer spacing in vertically aligned 2D $MoS_2$ upon $Li^+$ intercalation. Ability to externally modulate the electronic structures of 2D TMDs via such simple intercalation may open up substantially novel electrical and optical applications.

### 3.2.3 Thermoelectrics and photovoltaics

Intercalations have also been utilized to turn the materials properties of 2D materials to be suitable for energy conversion applications such as thermoelectrics or photovoltaics. In nanostructured thermoelectric materials, the general strategy to enhance thermoelectricity is to reduce thermal conductivity while maintaining electrical conductivity [71]. In 2D materials, this can be achieved by incorporating intercalants such as atoms, ions, molecules, and guest 2D layers into the van der Waals gaps of hosting 2D materials to perturb phonon propagation. In layered bulk materials, the intercalation of SnS into $TiS_2$ has been demonstrated to make SnS-$TiS_2$ superlattice which effectively reduces the transverse sound velocity owing due to enhanced interfaces [72]. Recent theory suggests that intercalation of foreign 2D layers

into hosting 2D $MoS_2$ can realize various $MoS_2$-based superlattice structures, effectively modifying their electronic structures [73]. Intercalating 2D layers further introduces structural disorder in the crystalline lattice of hosting 2D materials, resulting in efficient phonon localization. For example, electrochemical intercalations of $Li^+$ ions have been demonstrated to effectively modulate the thermal conductivity of lithium cobalt oxide ($LiCoO_2$), a layered crystal commonly used as cathode materials [74]. Such control of thermal conductivity can be generalized to various TMDs, stimulating an interest in designing novel hetero-structured thermoelectric materials inheriting their intriguing 2D nature [61]. In addition to thermoelectrics, intercalation can be employed to tune the materials properties of 2D TMDs to be suitable for photovoltaic applications. Hetero-structured 2D TMD composites such as $WS_2$/carbon-nanotubes and $WS_2$/graphene have been demonstrated by the intercalation-based exfoliation and integrations of dissimilar 2D materials [39, 75]. Considerable photoresponse has been observed in these materials, which is attributed to the efficient charge carrier separation due to the electronic junctions at the interfaces of dissimilar 2D materials. Figure 8 shows a schematic for the intercalation-based fabrication of $WS_2$/graphene photovoltaic devices (a) and the corresponding photoresponse upon illumination (b).

### 3.2.4 Magnetic properties and superconductivity

The Bridgman solid-state reaction, vapor transport and solution reaction intercalations can regulate the magnetic and superconducting properties of 2D TMDs, where the enhanced superconducting critical temperature ($T_C$) phenomena and large

magneto-resistive effect can be achieved [14, 17, 76]. Intercalated superconducting TMDs can pave a new way for enhancing the c-axis repeat distances to satisfy larger coherence distances of the superconducting wave function than interatomic distances, thus offering a basis for the study of low dimensional superconductivity [14]. In bulk layered materials, Geballe *et al.* reported that the intercalation of n-octadecylamine into $TaS_2$ achieved a large interlayer repeat distance of 5.7 nm, thus forming a large class of new superconductors by varying the certain intercalation molecules and the critical transition temperature can be enhanced to 5.3 K [17]. Recently, Clarke *et al.* reported lithium ions, lithium amide and ammonia intercalation into FeSe forming $Li_x(NH_2)_y(NH_3)_{1-y}Fe_2Se_2$ (x~0.6; y~0.2), exhibiting superconductivity at 43 K, higher than in any FeSe-derived compounds except the recent report of FeSe on $SrTiO_3$ [77, 78]. In the past decade, ultrathin 2D materials benefit from the intercalation chemistry for many applications. For the case of intercalated topological insulators, enhanced electric conductivity and conversion to superconductor have been observed in the $Cu_xBi_2Se_3$ systems. Figure 9(a) shows Cu intercalation into the van der Waals gap between $Bi_2Se_3$ layers. Transport measurements show superconductivity at 3.8 K in $Cu_xBi_2Se_3$ for $0.12 \leq x \leq 0.15$ (Figure 9b). The temperature-dependent resistivity yields an electron concentration (n-type) of $\sim 2 \times 10^{20}$ $cm^{-3}$ (Figure 9c), an order higher than intrinsic $Bi_2Se_3$, which is very different from the non-superconducting $Bi_{2-x}Cu_xSe_3$ crystals with $0 \leq x \leq 0.15$ [79]. Cava *et al.* also reported that Cu intercalation into $TiSe_2$ induce superconductivity in the range of $0.04 \leq x \leq 0.10$, proving a first opportunity for the study of charge density waves to superconductivity

transition [76]. As for the magnetic properties, by proper choice of intercalants, host materials and reaction stage, intercalated compounds can benefit from the spin dimensionality, non-magnetic layers and reduced interplanar magnetic coupling. As shown in Figure 8d, Morosan *at al.* reported Fe can be intercalated into $TaS_2$, forming the superlattice diffraction patterns. $Fe_{1/4}TaS_2$ orders ferromagnetically below 160 K and displays very sharp hysteresis loops in the ordered state when magnetic field is parallel to the c axis. For the case of $Fe_{0.28}TaS_2$, Figure 8e and 8f show the magnetoresistance measurements of bulk and exfoliated thin-crystals at selected temperatures. The different transition behavior of magnetoresistance curves between bulk (broadening) and 2D crystals (sharping) implies that long range coupling between the Fe ions in different layers is weaker in the 2D crystals. A remarkably large field-perpendicular-to-plane magnetoresistance (MR) exceeding 60% at 2 K was confirmed by anomalous Hall measurements [80, 81].

## 4. Outlook/Perspective

In this review, we have outlined that different strategies of intercalation chemistry pave an efficient way to the production of monolayer or few layer 2D TMDs, modulation of its crystal and band structure and tuning the physical and chemical properties of 2D TMDs. For the synthesis, the remaining challenges are improvement of crystal size, quality and mass production strategies with uniform physical and chemical properties, which can satisfy high performance electronic, optoelectronic, electrochemical catalyst and battery, biological applications[82]. For the physical

properties, intercalation reaction stage and intercalant species should give more rational designs for controlling the band structure, Fermi level and carrier density, for optimizing the superconducting temperature and for inducing magnetic properties. There is no doubt that intercalation chemistry still has an extensive space for 2D layered materials researchers toward study of high-quality new materials[83, 84], energy conversion devices and various physical, chemical, and biological properties.

**Acknowledgements**

J. J. C. acknowledges support from NSF MRSEC DMR 1119826. Y. Z. acknowledges support from NSF DMR 1402600. Y. J. acknowledges the startup fund from the University of Central Florida. All authors contribute to the manuscript.

References


1. S. M. Auerbach, K. A. Carrado and P. K. Dutta, *Handbook of layered materials*, CRC Press, 2004.
2. P. R. Wallace, *Physical Review*, 1947, **71**, 622-634.
3. R. W. Keyes, *Physical Review*, 1953, **92**, 580-584.
4. N. C. Norman, *Chemistry of arsenic, antimony and bismuth*, Springer Science & Business Media, 1998.
5. P. S. Braterman, Z. P. Xu and F. Yarberry, *Handbook of layered materials*, 2004, 373-474.
6. C. H. Lee, T. Schiros, E. J. G. Santos, B. Kim, K. G. Yager, S. J. Kang, S. Lee, J. Yu, K. Watanabe, T. Taniguchi, J. Hone, E. Kaxiras, C. Nuckolls and P. Kim, *Advanced Materials*, 2014, **26**, 2812-2817.
7. D. W. He, Y. A. Zhang, Q. S. Wu, R. Xu, H. Y. Nan, J. F. Liu, J. J. Yao, Z. L. Wang, S. J. Yuan, Y. Li, Y. Shi, J. L. Wang, Z. H. Ni, L. He, F. Miao, F. Q. Song, H. X. Xu, K. Watanabe, T. Taniguchi, J. B. Xu and X. R. Wang, *Nature Communications*, 2014, **5**, 5162.
8. M. Chhowalla, H. S. Shin, G. Eda, L. J. Li, K. P. Loh and H. Zhang, *Nature Chemistry*, 2013, **5**, 263-275.
9. J. J. Cha and Y. Cui, *Nature Nanotechnology*, 2012, **7**, 85-86.
10. H. L. Peng, K. J. Lai, D. S. Kong, S. Meister, Y. L. Chen, X. L. Qi, S. C. Zhang, Z. X. Shen and Y. Cui, *Nature Materials*, 2010, **9**, 225-229.
11. Y. H. Li, J. L. Huang and C. M. Lieber, *Physical Review Letters*, 1992, **68**, 3240-3243.
12. M. Chhowalla, Z. F. Liu and H. Zhang, *Chemical Society Reviews*, 2015, **44**, 2584-2586.
13. H. T. Yuan, H. T. Wang and Y. Cui, *Accounts of Chemical Research*, 2015, **48**, 81-90.
14. M. Dresselhaus, *MRS Bulletin*, 1987, **12**, 24-28.
15. M. S. Dresselhaus, *Physics Today*, 2008, **37**, 60-68.
16. X. Huang, Z. Zeng and H. Zhang, *Chemical Society Reviews*, 2013, **42**, 1934-1946.
17. F. R. Gamble, J. H. Osiecki, M. Cais and Pisharod.R, *Science*, 1971, **174**, 493.
18. D. E. Prober, M. R. Beasley and R. E. Schwall, *Physical Review B*, 1977, **15**, 5245-5261.
19. F. Bonaccorso, Z. Sun, T. Hasan and A. C. Ferrari, *Nature Photonics*, 2010, **4**, 611-622.
20. Y. Jung, J. Shen and J. J. Cha, *Nano Convergence*, 2014, **1**, 1-8.
21. B. Radisavljevic, A. Radenovic, J. Brivio, V. Giacometti and A. Kis, *Nature Nanotechnology*, 2011, **6**, 147-150.
22. O. Lopez-Sanchez, D. Lembke, M. Kayci, A. Radenovic and A. Kis, *Nature Nanotechnology*, 2013, **8**, 497-501.

23. W. Z. Wu, L. Wang, Y. L. Li, F. Zhang, L. Lin, S. M. Niu, D. Chenet, X. Zhang, Y. F. Hao, T. F. Heinz, J. Hone and Z. L. Wang, *Nature*, 2014, **514**, 470.
24. H. Y. Zhu, Y. Wang, J. Xiao, M. Liu, S. M. Xiong, Z. J. Wong, Z. L. Ye, Y. Ye, X. B. Yin and X. Zhang, *Nature Nanotechnology*, 2015, **10**, 151-155.
25. D. Voiry, H. Yamaguchi, J. W. Li, R. Silva, D. C. B. Alves, T. Fujita, M. W. Chen, T. Asefa, V. B. Shenoy, G. Eda and M. Chhowalla, *Nature Materials*, 2013, **12**, 850-855.
26. K. F. Mak, C. Lee, J. Hone, J. Shan and T. F. Heinz, *Physical Review Letters*, 2010, **105**.
27. T. Cao, G. Wang, W. P. Han, H. Q. Ye, C. R. Zhu, J. R. Shi, Q. Niu, P. H. Tan, E. Wang, B. L. Liu and J. Feng, *Nature Communications*, 2012, **3**, 887.
28. K. F. Mak, K. L. He, J. Shan and T. F. Heinz, *Nature Nanotechnology*, 2012, **7**, 494-498.
29. H. T. Wang, Z. Y. Lu, S. C. Xu, D. S. Kong, J. J. Cha, G. Y. Zheng, P. C. Hsu, K. Yan, D. Bradshaw, F. B. Prinz and Y. Cui, *Proceedings of the National Academy of Sciences of the United States of America*, 2013, **110**, 19701-19706.
30. D. S. Kong, H. T. Wang, J. J. Cha, M. Pasta, K. J. Koski, J. Yao and Y. Cui, *Nano Letters*, 2013, **13**, 1341-1347.
31. Y. Jung, J. Shen, Y. Sun and J. J. Cha, *ACS nano*, 2014, **8**, 9550-9557.
32. Y. Jung, J. Shen, Y. Liu, J. M. Woods, Y. Sun and J. J. Cha, *Nano Letters*, 2014, **14**, 6842-6849.
33. T. Georgiou, R. Jalil, B. D. Belle, L. Britnell, R. V. Gorbachev, S. V. Morozov, Y.-J. Kim, A. Gholinia, S. J. Haigh and O. Makarovsky, *Nature Nanotechnology*, 2013, **8**, 100-103.
34. L. Britnell, R. M. Ribeiro, A. Eckmann, R. Jalil, B. D. Belle, A. Mishchenko, Y. J. Kim, R. V. Gorbachev, T. Georgiou, S. V. Morozov, A. N. Grigorenko, A. K. Geim, C. Casiraghi, A. H. Castro Neto and K. S. Novoselov, *Science*, 2013, **340**, 1311-1314.
35. M. M. Furchi, A. Pospischil, F. Libisch, J. Burgdorfer and T. Mueller, *Nano Letters*, 2014, **14**, 4785-4791.
36. J. S. Ross, P. Klement, A. M. Jones, N. J. Ghimire, J. Q. Yan, D. G. Mandrus, T. Taniguchi, K. Watanabe, K. Kitamura, W. Yao, D. H. Cobden and X. D. Xu, *Nature Nanotechnology*, 2014, **9**, 268-272.
37. C. M. Huang, S. F. Wu, A. M. Sanchez, J. J. P. Peters, R. Beanland, J. S. Ross, P. Rivera, W. Yao, D. H. Cobden and X. D. Xu, *Nature Materials*, 2014, **13**, 1096-1101.
38. K. S. Novoselov, A. K. Geim, S. V. Morozov, D. Jiang, Y. Zhang, S. V. Dubonos, I. V. Grigorieva and A. A. Firsov, *Science*, 2004, **306**, 666-669.
39. J. N. Coleman, M. Lotya, A. O'Neill, S. D. Bergin, P. J. King, U. Khan, K. Young, A. Gaucher, S. De, R. J. Smith, I. V. Shvets, S. K. Arora, G. Stanton, H. Y. Kim, K. Lee, G. T. Kim, G. S. Duesberg, T. Hallam, J. J. Boland, J. J. Wang, J. F. Donegan, J. C. Grunlan, G. Moriarty, A. Shmeliov, R. J. Nicholls,

J. M. Perkins, E. M. Grieveson, K. Theuwissen, D. W. McComb, P. D. Nellist and V. Nicolosi, *Science*, 2011, **331**, 568-571.
40. V. Nicolosi, M. Chhowalla, M. G. Kanatzidis, M. S. Strano and J. N. Coleman, *Science*, 2013, **340**, 1420.
41. S. Park and R. S. Ruoff, *Nature Nanotechnology*, 2009, **4**, 217-224.
42. D. A. Dikin, S. Stankovich, E. J. Zimney, R. D. Piner, G. H. B. Dommett, G. Evmenenko, S. T. Nguyen and R. S. Ruoff, *Nature*, 2007, **448**, 457-460.
43. D. R. Dreyer, S. Park, C. W. Bielawski and R. S. Ruoff, *Chemical Society Reviews*, 2010, **39**, 228-240.
44. M. Osada and T. Sasaki, *Journal of Materials Chemistry*, 2009, **19**, 2503-2511.
45. M. M. J. Treacy, S. B. Rice, A. J. Jacobson and J. T. Lewandowski, *Chemistry of Materials*, 1990, **2**, 279-286.
46. C. J. Shih, A. Vijayaraghavan, R. Krishnan, R. Sharma, J. H. Han, M. H. Ham, Z. Jin, S. C. Lin, G. L. C. Paulus, N. F. Reuel, Q. H. Wang, D. Blankschtein and M. S. Strano, *Nature Nanotechnology*, 2011, **6**, 439-445.
47. G. Eda, H. Yamaguchi, D. Voiry, T. Fujita, M. W. Chen and M. Chhowalla, *Nano Letters*, 2011, **11**, 5111-5116.
48. A. A. Jeffery, C. Nethravathi and M. Rajamathi, *Journal of Physical Chemistry C*, 2014, **118**, 1386-1396.
49. A. A. Jeffery, C. Nethravathi and M. Rajamathi, *Rsc Advances*, 2015, **5**, 51176-51182.
50. Q. Liu, X. L. Li, Z. R. Xiao, Y. Zhou, H. P. Chen, A. Khalil, T. Xiang, J. Q. Xu, W. S. Chu, X. J. Wu, J. L. Yang, C. M. Wang, Y. J. Xiong, C. H. Jin, P. M. Ajayan and L. Song, *Advanced Materials*, 2015, **27**, 4837-4844.
51. J. Zheng, H. Zhang, S. H. Dong, Y. P. Liu, C. T. Nai, H. S. Shin, H. Y. Jeong, B. Liu and K. P. Loh, *Nature Communications*, 2014, **5**.2995.
52. K. J. Koski, C. D. Wessells, B. W. Reed, J. J. Cha, D. S. Kong and Y. Cui, *Journal of the American Chemical Society*, 2012, **134**, 13773-13779.
53. J. P. Motter, K. J. Koski and Y. Cui, *Chemistry of Materials*, 2014, **26**, 2313-2317.
54. K. J. Koski, J. J. Cha, B. W. Reed, C. D. Wessells, D. S. Kong and Y. Cui, *Journal of the American Chemical Society*, 2012, **134**, 7584-7587.
55. M. J. Wang and K. J. Koski, *Acs Nano*, 2015, **9**, 3226-3233.
56. K. P. Chen, F. R. Chung, M. J. Wang and K. J. Koski, *Journal of the American Chemical Society*, 2015, **137**, 5431-5437.
57. Z. Y. Zeng, Z. Y. Yin, X. Huang, H. Li, Q. Y. He, G. Lu, F. Boey and H. Zhang, *Angewandte Chemie-International Edition*, 2011, **50**, 11093-11097.
58. H. L. Peng, X. F. Zhang, R. D. Twesten and Y. Cui, *Nano Research*, 2009, **2**, 327-335.
59. D. Voiry, M. Salehi, R. Silva, T. Fujita, M. W. Chen, T. Asefa, V. B. Shenoy, G. Eda and M. Chhowalla, *Nano Letters*, 2013, **13**, 6222-6227.
60. R. Kappera, D. Voiry, S. E. Yalcin, B. Branch, G. Gupta, A. D. Mohite and M. Chhowalla, *Nature Materials*, 2014, **13**, 1128-1134.

61. H. T. Wang, H. T. Yuan, S. S. Hong, Y. B. Li and Y. Cui, *Chemical Society Reviews*, 2015, **44**, 2664-2680.
62. M. A. Lukowski, A. S. Daniel, F. Meng, A. Forticaux, L. S. Li and S. Jin, *Journal of the American Chemical Society*, 2013, **135**, 10274-10277.
63. H. T. Wang, Z. Y. Lu, D. S. Kong, J. Sun, T. M. Hymel and Y. Cui, *Acs Nano*, 2014, **8**, 4940-4947.
64. Z. Y. Lu, H. T. Wang, D. S. Kong, K. Yan, P. C. Hsu, G. Y. Zheng, H. B. Yao, Z. Liang, X. M. Sun and Y. Cui, *Nature Communications*, 2014, **5**.43435.
65. G. D. Du, Z. P. Guo, S. Q. Wang, R. Zeng, Z. X. Chen and H. K. Liu, *Chemical Communications*, 2010, **46**, 1106-1108.
66. J. Xiao, D. W. Choi, L. Cosimbescu, P. Koech, J. Liu and J. P. Lemmon, *Chemistry of Materials*, 2010, **22**, 4522-4524.
67. Q. Liu, X. L. Li, Q. He, A. Khalil, D. B. Liu, T. Xiang, X. J. Wu and L. Song, *Small*, 2015, **11**, 5556-5564.
68. J. J. Cha, K. J. Koski, K. C. Y. Huang, K. X. Wan, W. D. Luo, D. S. Kong, Z. F. Yu, S. H. Fan, M. L. Brongersma and Y. Cui, *Nano Letters*, 2013, **13**, 5913-5918.
69. J. Yao, K. J. Koski, W. D. Luo, J. J. Cha, L. B. Hu, D. S. Kong, V. K. Narasimhan, K. F. Huo and Y. Cui, *Nature Communications*, 2014, **5**.5670.
70. W. Z. Bao, J. Y. Wan, X. G. Han, X. H. Cai, H. L. Zhu, D. H. Kim, D. K. Ma, Y. L. Xu, J. N. Munday, H. D. Drew, M. S. Fuhrer and L. B. Hu, *Nature Communications*, 2014, **5**.4224.
71. M. S. Dresselhaus, G. Chen, M. Y. Tang, R. G. Yang, H. Lee, D. Z. Wang, Z. F. Ren, J. P. Fleurial and P. Gogna, *Advanced Materials*, 2007, **19**, 1043-1053.
72. C. L. Wan, Y. F. Wang, N. Wang, W. Norimatsu, M. Kusunoki and K. Koumoto, *Journal of Electronic Materials*, 2011, **40**, 1271-1280.
73. N. Lu, H. Y. Guo, L. Wang, X. J. Wu and X. C. Zeng, *Nanoscale*, 2014, **6**, 4566-4571.
74. J. Cho, M. D. Losego, H. G. Zhang, H. Kim, J. M. Zuo, I. Petrov, D. G. Cahill and P. V. Braun, *Nature Communications*, 2014, **5**.4083.
75. F. Withers, H. Yang, L. Britnell, A. P. Rooney, E. Lewis, A. Felten, C. R. Woods, V. S. Romaguera, T. Georgiou, A. Eckmann, Y. J. Kim, S. G. Yeates, S. J. Haigh, A. K. Geim, K. S. Novoselov and C. Casiraghi, *Nano Letters*, 2014, **14**, 3987-3992.
76. E. Morosan, H. W. Zandbergen, B. S. Dennis, J. W. G. Bos, Y. Onose, T. Klimczuk, A. P. Ramirez, N. P. Ong and R. J. Cava, *Nature Physics*, 2006, **2**, 544-550.
77. M. Burrard-Lucas, D. G. Free, S. J. Sedlmaier, J. D. Wright, S. J. Cassidy, Y. Hara, A. J. Corkett, T. Lancaster, P. J. Baker, S. J. Blundell and S. J. Clarke, *Nature Materials*, 2013, **12**, 15-19.
78. J. F. Ge, Z. L. Liu, C. H. Liu, C. L. Gao, D. Qian, Q. K. Xue, Y. Liu and J. F. Jia, *Nature Materials*, 2015, **14**, 285-289.

79. Y. S. Hor, A. J. Williams, J. G. Checkelsky, P. Roushan, J. Seo, Q. Xu, H. W. Zandbergen, A. Yazdani, N. P. Ong and R. J. Cava, *Physical Review Letters*, 2010, **104**.057001.
80. E. Morosan, H. W. Zandbergen, L. Li, M. Lee, J. G. Checkelsky, M. Heinrich, T. Siegrist, N. P. Ong and R. J. Cava, *Physical Review B*, 2007, **75**.104401.
81. W. J. Hardy, C. W. Chen, A. Marcinkova, H. Ji, J. Sinova, D. Natelson and E. Morosan, *Physical Review B*, 2015, **91**. 054426.
82. Q. Liu, C. Sun, Q. He, A. Khalil, T. Xiang, D. Liu, Y. Zhou, J. Wang and L. Song, *Nano Research*, 2015, **8**, 3982-3991.
83. W. W. Xiong, J. W. Miao, K. Q. Ye, Y. Wang, B. Liu and Q. C. Zhang, *Angewandte Chemie-International Edition*, 2015, **54**, 546-550.
84. C. L. Wan, X. K. Gu, F. Dang, T. Itoh, Y. F. Wang, H. Sasaki, M. Kondo, K. Koga, K. Yabuki, G. J. Snyder, R. G. Yang and K. Koumoto, *Nature Materials*, 2015, **14**, 622-627.

## Figure captions

**Figure 1**. Schematic for intercalation in the TMDs-type layered materials, where guest species can be inserted into van der Waals gap by diverse methods.

**Figure 2**. (a) Schematic for ion exchange intercalation of 2D TMDs. Some layered materials contain ions between 2D layers so as to balance surface charge on the layers. These ions (red spheres) can be exchanged for other ions (yellow spheres) in a liquid environment (from ref [40]). (b-d) Large-yield exfoliation of 2D $MoS_2$ and other TMDs via $N_2H_4$ intercalations. (b) Bulk $MoS_2$ reacts with $N_2H_4$, resulting in swollen 2D layers. (c) The reacted $MoS_2$ subsequently intercalates with alkali naphthalenide solution ($A^+$ $C_{10}H^-_8$) and then exfoliates to single $MoS_2$ layers. (d) Large-scale exfoliation of other TMDs; $TiS_2$ (left) $TaS_2$ (mid) $NbS_2$ (right) (from ref [51])

**Figure 3**. (a) Schematic for zerovalent metals intercalation into 2D TMDs. (from ref [53]). (b) Electron diffraction patterns of $Bi_2Se_3$ upon Cu intercalation, showing a variety of superlattice structures accommodating nearly 60 % of Cu (from ref [54])

**Figure 4**. (a) Schematic for the electrochemical Li+ intercalation of 2D TMDs. (b) Transmission electron (TEM) micrograph of a single layer $MoS_2$ exfoliated from the Li+ intercalation. (b) High-resolution TEM (HRTEM) of a single layer $MoS_2$ (top) and its corresponding electron diffraction (bottom) (from ref [57])

**Figure 5.** (a) Schematic for the transition of 2H phase to 1T phase in $MoS_2$ upon $Li^+$ intercalation. (b) Enhanced catalytic performance of 1T $MoS_2$ over 2H $MoS_2$. (from ref [62] )

**Figure 6**. (a,b) Tuning the optical properties of $Bi_2Se_3$ nanoplates via Cu intercalation. (a) Optical transmission image of an 8-nm thick $Bi_2Se_3$ nanoplates before (left) and after (right) Cu intercalations. Scale bar, 4 μm. (b) Optical transmission spectra of $Bi_2Se_3$ nanoplates with various thicknesses before (black) and after (red) Cu intercalations. (c,d) Tuning the electrical properties of $Bi_2Se_3$ nanoplates via Cu intercalation. (c) A $Bi_2Se_3$ nanoplate-based four-point probe measurement device on silicon substrate. Scale bar, 5 μm. (d) Sheet resistance of $Bi_2Se_3$ nanoplates with various thicknesses before (black) and after (red) Cu intercalations. (from ref [69])

**Figure 7**. Li+ intercalation driven-change of 2D $MoS_2$ interlayer spacing. (a-e) TEM images of $MoS_2$ with 2D molecular layers perpendicular to the substrate (a) before intercalation. (b-e) after intercalation to 1.8, 1.5, 1.2, and 1.1 V vs. Li+/Li, respectively. (f) Averaged layer spacing of pristine and lithiated $MoS_2$. Scale bar, 10 nm. (from ref [29])

**Figure 8.** (a) Schematic for a fabrication of general heterostructures prepared by using 2D-materials solutions. (b) Photoresponsivity of a WS2/graphene device as a function of back gate. (from ref [75])

**Figure 9.** (a) Schematic for the crystal structure of Cu intercalated $Bi_2Se_3$. (b) The temperature-dependent magnetic transport measurements of a single crystal of $Cu_{0.12}Bi_2Se_3$, showing a superconducting transition Tc~3.8 K from the zero-field-cooled (ZFC) and field-cooled (FC) measurements. (c) The temperature-dependent resistivity of a $Cu_{0.12}Bi_2Se_3$ crystal with applied current in the ab plane. (from ref [79]) (d) Schematic for Schematic for the crystal structure of $Fe_{1/4}TaS_2$. (e, f) Magnetoresistance measurements of bulk and exfoliated thin $Fe_{0.28}TaS_2$ crystals at selected temperatures for H∥ c axis, and i ∥ ab-plane. (from ref [80, 81])

.

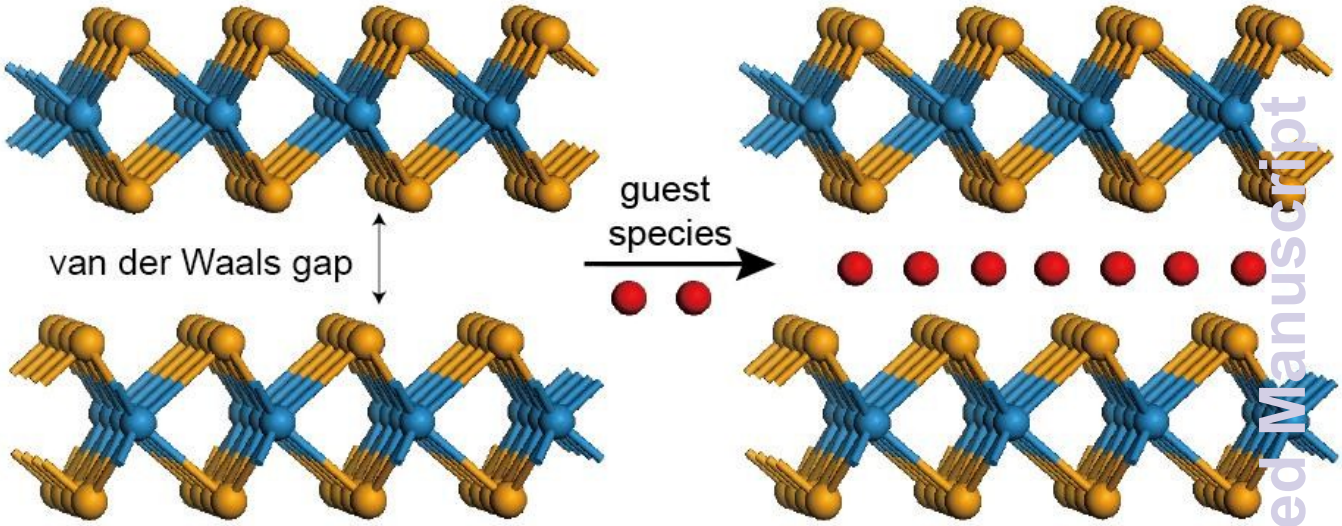


Figure 1

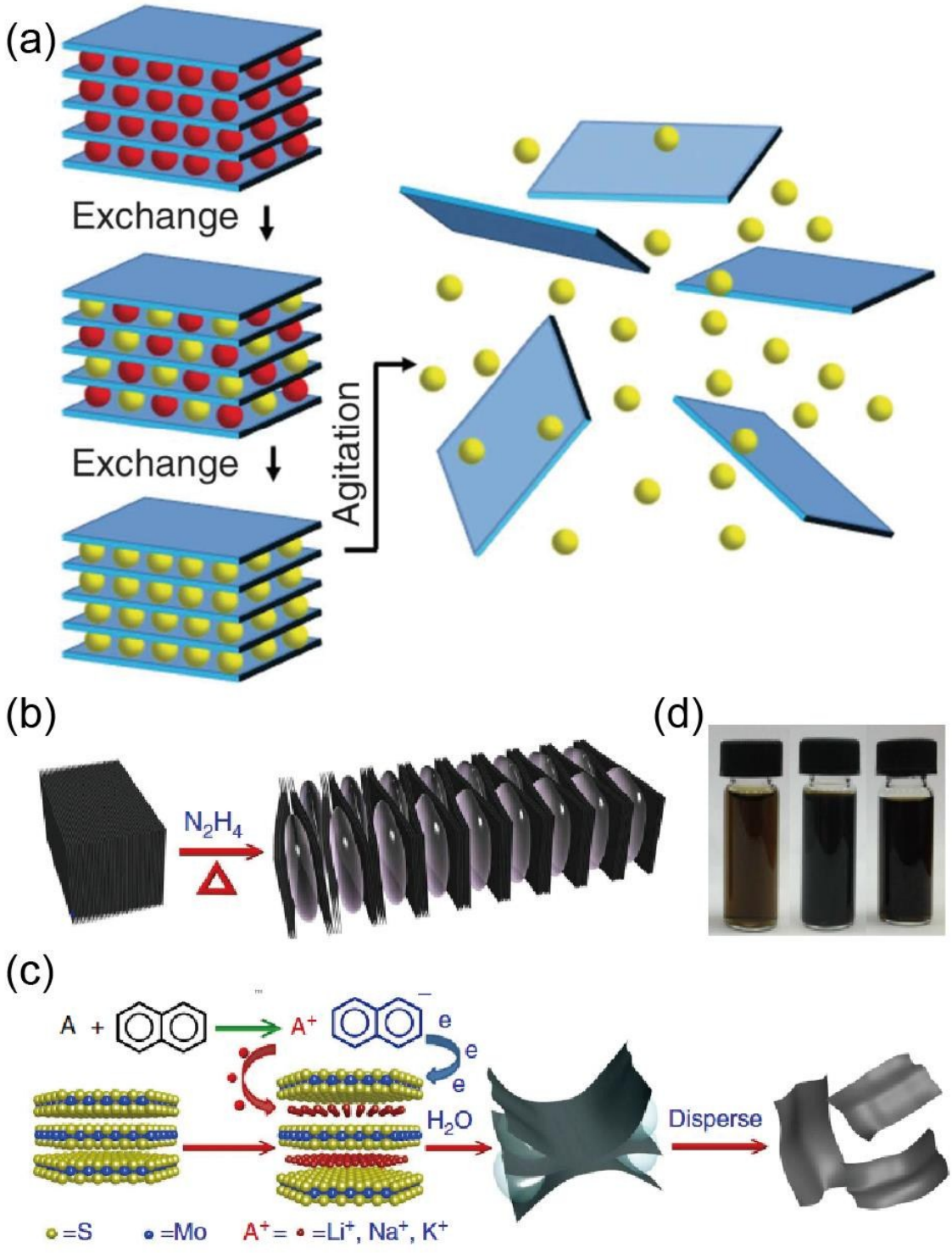


Figure 2

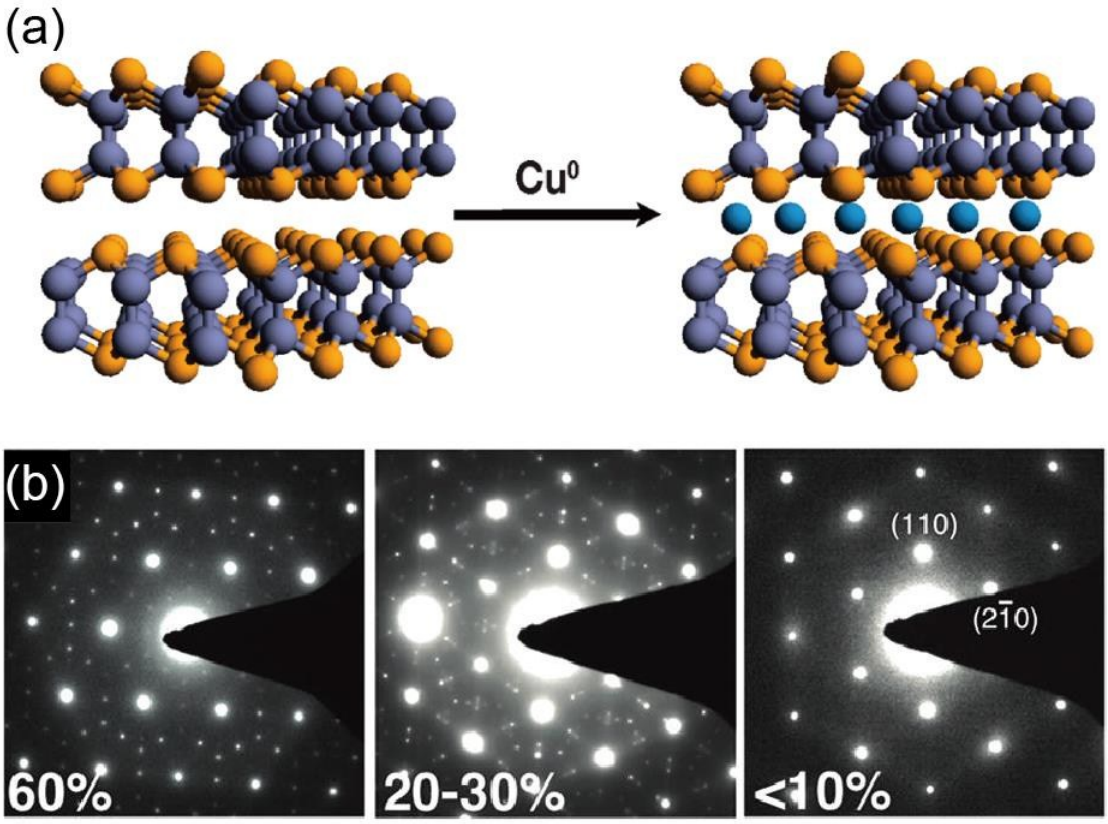


Figure 3

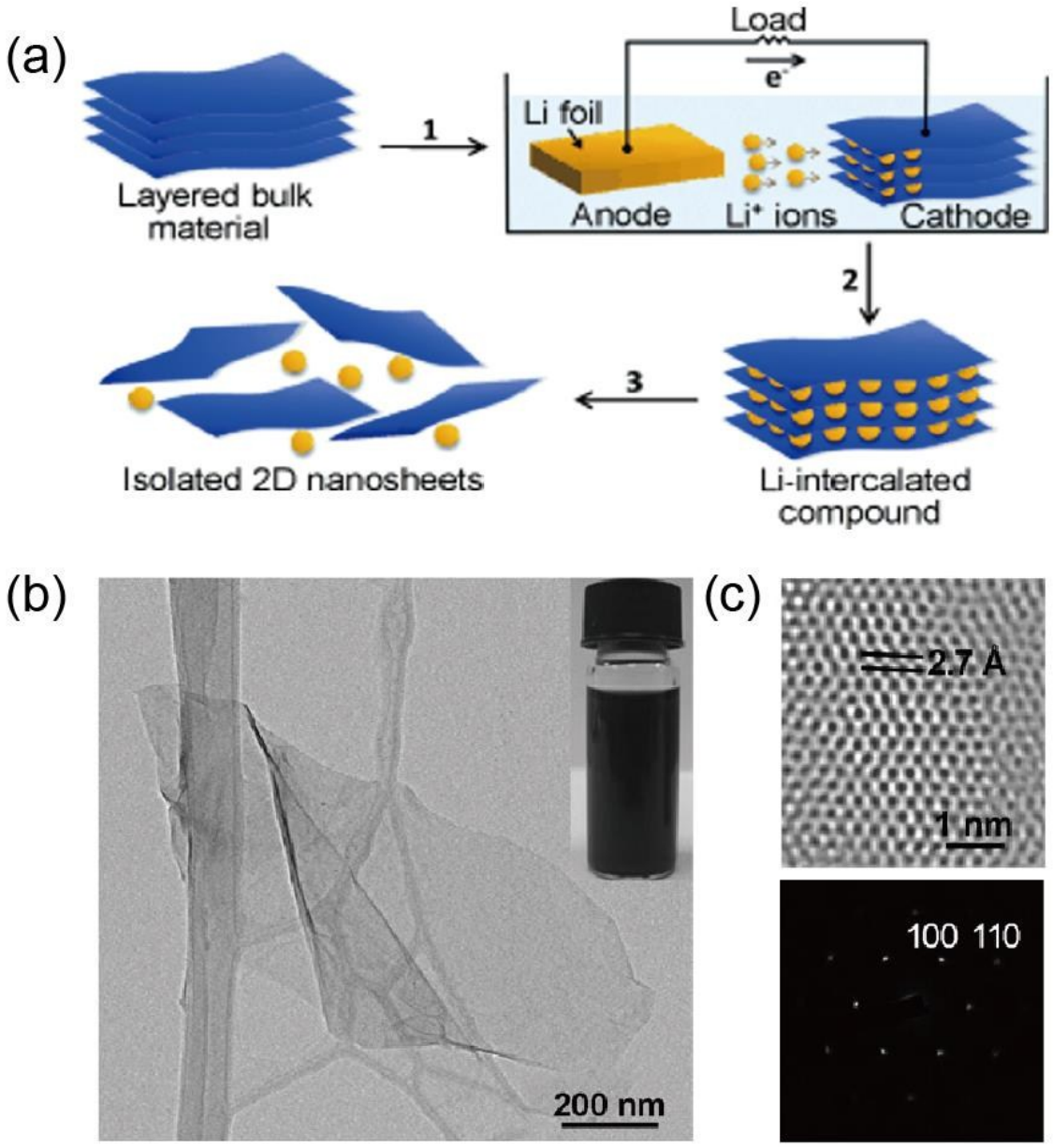


Figure 4

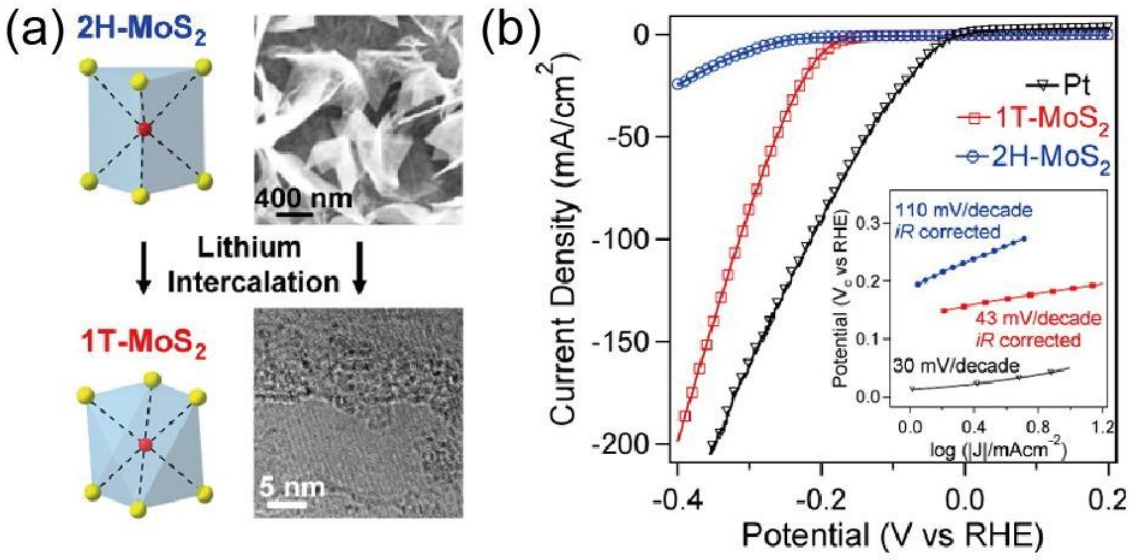


Figure 5

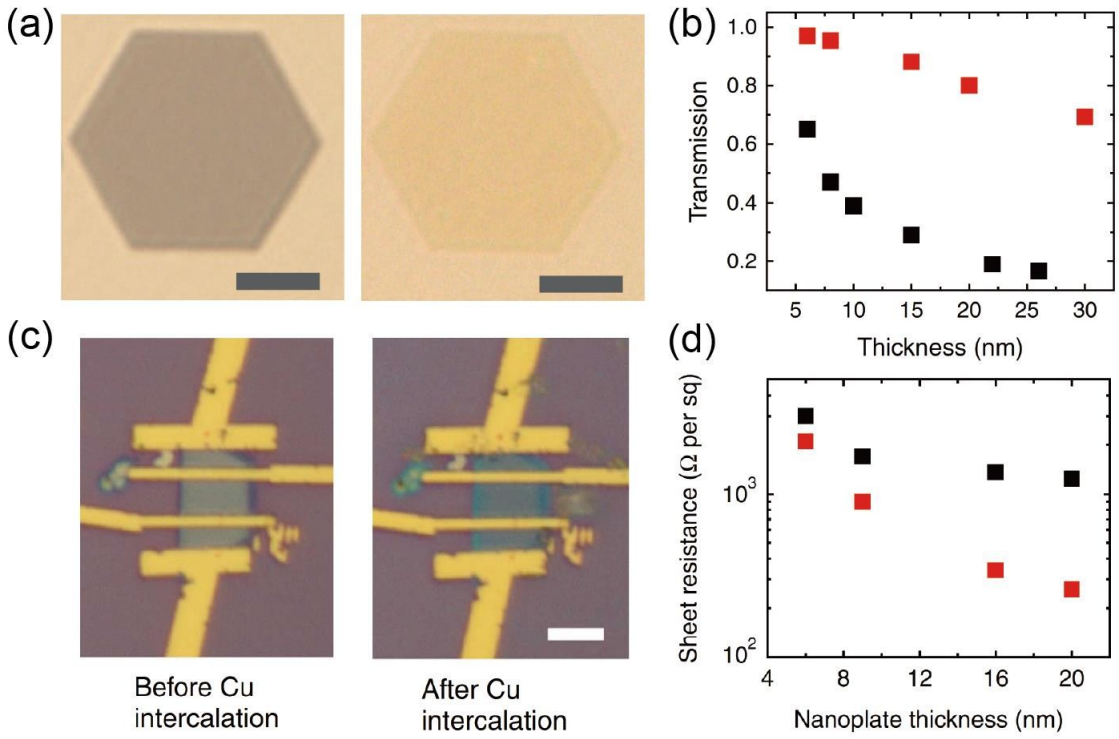


Figure 6

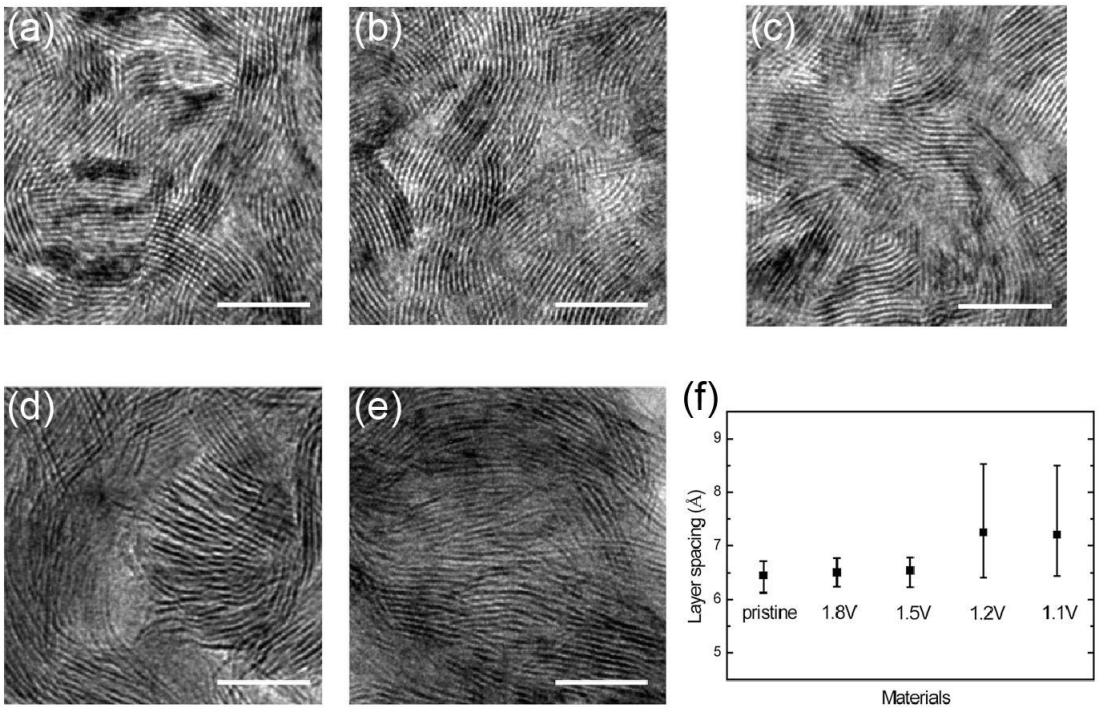


Figure 7

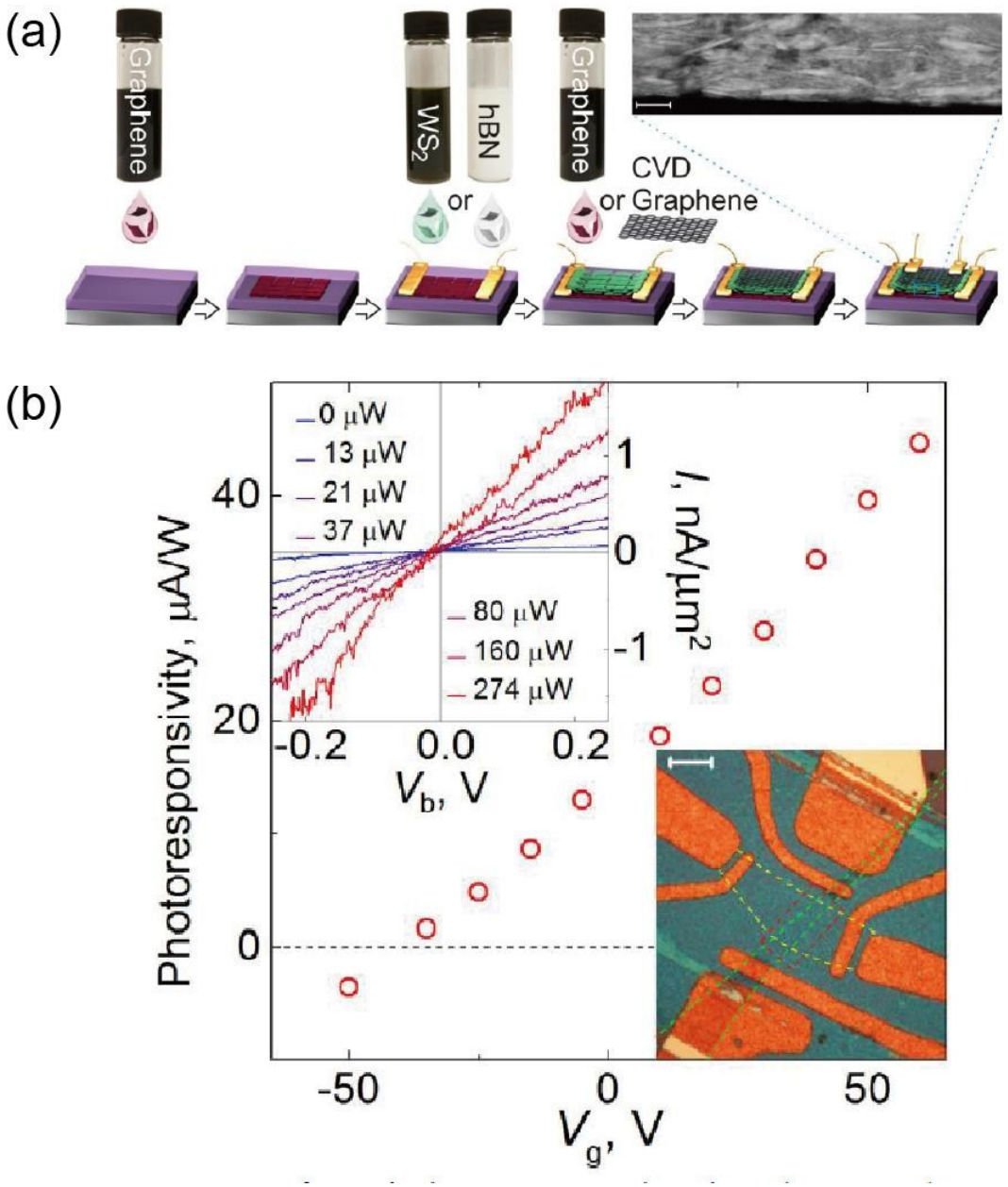


Figure 8

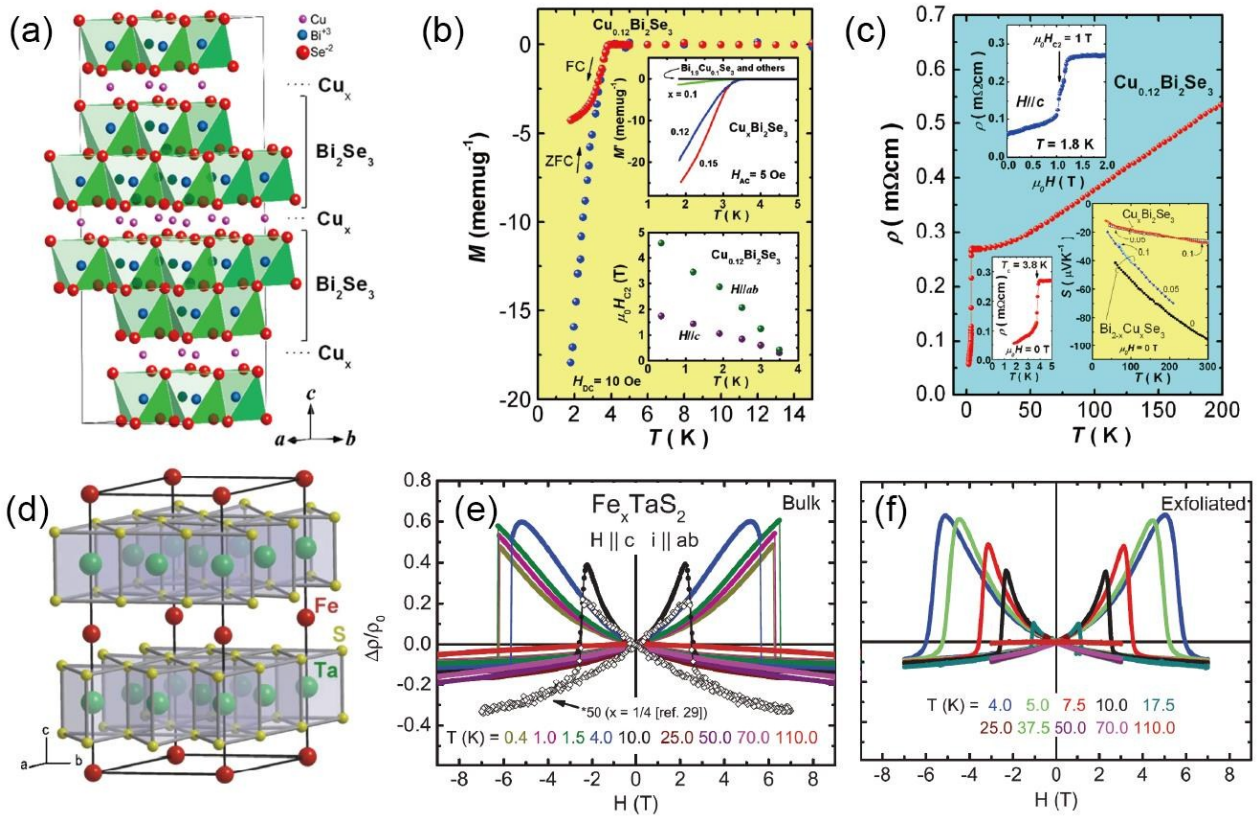


Figure 9